Supplementary Material for Dang *et al.*

Thaumarchaeotal Signature Gene Distribution in Sediments of the Northern South China Sea – an indicator for the metabolic intersection of the marine carbon, nitrogen and phosphorus cycles?

Hongyue Dang,[a,b,#] Haixia Zhou,[a] Jinying Yang,[a] Huangmin Ge,[c] Nianzhi Jiao,[b] Xiwu Luan,[d,e] Chuanlun Zhang,[c,#] and Martin G. Klotz[a,f]

State Key Laboratory of Heavy Oil Processing, Key Laboratory of Bioengineering and Biotechnology in Universities of Shandong, Centre for Bioengineering and Biotechnology, China University of Petroleum (East China), Qingdao 266580, China[a]; State Key Laboratory of Marine Environmental Science, Xiamen University, Xiamen 361005, China[b]; State Key Laboratory of Marine Geology, Tongji University, Shanghai 200092, China[c]; Key Laboratory of Marine Hydrocarbon Resources and Environmental Geology, Ministry of Land and Resources of China, Qingdao 266071, China[d]; Qingdao Institute of Marine Geology, Qingdao 266071, China[e]; and Department of Biology, University of North Carolina, Charlotte, NC 28223, USA[f]

This material includes a table of the *in situ* environmental parameter measurements (Table S1), a table of PCR and qPCR primers and thermal profiles of the target genes (Table S2), a table of qPCR efficiency and sensitivity of each of the target genes measured (Table S3), a table showing the diversity and predicted richness of the sediment thaumarchaeotal *amoA* gene sequences obtained from the nSCS (Table S4), a table of Pearson correlation analysis results (Table S5), a table of surface sediment microbial membrane core lipid measurements (Table S6), a figure showing the map of the northern South China Sea and the geographical locations of our sampling sites (Fig. S1), a figure showing the Fast UniFrac environment clustering dendrogram with replicate A3 subcore sediment samples (Fig. S2), a figure showing the Fast UniFrac PCoA ordination diagram with replicate A3 subcore sediment samples (Fig. S3), a figure showing the *amoA* gene clone libraries' rarefaction curves (Fig. S4), a figure showing the Fast UniFrac environment clustering dendrogram (Fig. S5), a figure showing the distribution of the BIT values in the nSCS sampling sites (Fig. S6), a figure showing the dendrogram of the hierarchical clustering analysis of the nSCS sediment putative fossil archaeal assemblages constructed using the archaeal membrane core lipid data (Fig. S7), and a figure showing the phylogeny of the Thaumarchaeota PstA protein sequences (Fig. S8).

Table S1. The measurements of *in situ* environmental parameters of the 12 sampling stations in the nSCS[a].

Environmental factor	Station											
	A3	**CF6**	**CF8**	**CF11**	**CF14**	**CF15**	**E407**	**E422**	**E501**	**E504**	**E505**	**E801**
Longitude (°E)	114º23.163’	119º30.060’	111º3.710’	114º34.477’	115º12.971’	115º29.373’	120º0.017’	112º0.793’	110º41.835’	111º18.096’	111º29.029’	110º20.410’
Latitude (°N)	21º50.525’	22º0.316’	18º1.908’	19º43.341’	19º54.256’	19º59.581’	18º29.810’	18º0.341’	18º59.995’	19º0.102’	18º59.897’	17º11.450’
Water depth (m)	52	2441	1548	1050	1220	1300	1800	2456	65	131	154	1400.
Sediment												
Temperature (°C)	21.9	5.5	5.0	5.2	3.6	3.4	4.7	3.8	20.5	17.7	17.4	3.8
WC (water content, %)	36.92	29.66	27.92	32.25	33.19	36.40	32.51	32.37	18.23	35.22	15.22	27.94
OM (organic matter, %)	1.89	3.06	2.26	2.10	1.83	2.68	2.33	2.09	1.08	1.79	1.58	3.22
OrgC (organic C, %)	1.00	0.63	0.96	1.32	1.32	1.27	0.67	0.94	0.28	0.76	0.47	1.09
OrgN (organic N, %)	0.10	0.08	0.12	0.16	0.15	0.17	0.06	0.11	0.03	0.08	0.06	0.14
OrgP (organic P, μmol/g)	5.92	3.52	6.17	8.69	7.62	12.62	8.36	4.28	3.11	6.31	2.55	8.55
IP (inorganic P, μmol/g)	19.89	23.52	16.56	17.53	16.56	13.99	16.31	18.64	7.81	17.61	15.33	15.23
TP (total P, μmol/g)	25.81	27.04	22.73	26.22	24.18	26.61	24.67	22.92	10.92	23.92	17.88	23.78
OrgC/OrgN	10.00	7.88	8.00	8.25	8.80	7.47	11.17	8.55	9.33	9.50	7.83	7.79
Sand content (%)	0.00	0.00	0.00	0.00	0.00	0.00	0.00	0.00	38.18	0.14	0.62	0.00
Silt content (%)	64.91	63.00	62.93	62.41	62.74	60.75	53.61	59.29	44.46	69.72	75.7	57.94
Clay content (%)	35.09	36.97	37.07	37.59	37.26	39.25	46.39	40.71	17.37	30.14	23.68	42.06
Median grain size (ø)	7.00	7.27	7.12	7.14	7.15	7.28	7.78	7.34	4.75	6.68	6.12	7.58
Mean grain size (ø)	7.27	7.49	7.42	7.42	7.37	7.48	7.74	7.61	5.43	7.01	6.52	7.71
Sorting coefficient	1.65	1.50	1.59	1.60	1.63	1.60	1.56	1.54	2.25	1.69	1.79	1.40
Kurtosis	1.95	1.80	1.86	1.88	1.92	1.88	1.85	1.78	2.74	2.02	2.18	1.65
Skewness	0.95	0.84	0.97	0.93	0.87	0.78	-0.76	0.88	1.94	1.17	1.49	0.78
Sediment pore-water												
Salinity (‰)	31.5	31.2	31.0	30.0	30.5	31.5	31.5	30.0	30.1	31.0	32.5	31.0
pH	7.17	7.11	7.40	7.16	7.15	7.15	7.06	7.17	7.28	7.13	7.35	7.06
Eh (mv)	-15.0	-11.0	-28.0	-14.0	-13.0	-13.0	-8.0	-14.0	-21.0	-12.0	-27.0	-8.0
DO (μM)	118.75	203.13	128.13	178.13	237.50	140.63	237.50	234.38	115.63	96.88	165.63	215.63
NO_3^- (μM)	14.31	3.61	1.46	13.58	14.92	6.43	22.67	17.42	3.95	2.85	6.30	9.05
NO_2^- (μM)	0.42	0.83	0.60	1.09	1.19	1.00	1.86	1.53	0.63	2.80	0.56	3.99
NO_x^- (μM)[b]	14.73	4.44	2.06	14.67	16.11	7.43	24.53	18.95	4.58	5.65	6.86	13.04
NH_4^+ (μM)	47.11	5.97	54.25	8.22	105.94	13.76	126.68	8.72	525.74	59.11	32.70	475.56
DIN (μM)[c]	61.84	10.41	56.31	22.89	122.05	21.19	151.21	27.67	530.32	64.76	39.56	488.60
PO_4^{3-} (μM)	5.49	6.26	6.42	7.54	6.19	6.29	8.46	7.62	5.07	9.08	4.42	14.42
N/P (DIN/ PO_4^{3-})	11.26	1.66	8.77	3.04	19.72	3.37	17.87	3.63	104.60	7.13	8.95	33.88
Urea (μM)	1.91	1.00	1.24	1.16	2.07	2.82	0.58	1.58	2.41	1.33	2.57	5.06

[a] Environmental factor measurements have been performed previously (Dang *et al*., 2013).
[b] NO_x^- was calculated as the sum of NO_2^- and NO_3^-.
[c] The total inorganic N concentration (DIN) was calculated as the sum of NH_4^+, NO_2^- and NO_3^-.

REFERENCE

Dang HY, Yang JY, Li J, Luan XW, Zhang YB, Gu GZ, Xue RR, Zong MY, Klotz MG. 2013. Environment-dependent distribution of the sediment *nifH*-harboring microbiota in the northern South China Sea. Appl. Environ. Microbiol. **79:**121-132.

Table S2. Primers and thermal profiles used for cloning PCR and qPCR quantifications of different genes.

Target Gene	Primer and sequence	PCR Type	Thermal Profile	Reference
Thaumarchaeota *amoA*	Arch-amoAF: 5'-STAATGGTCTGGCTTAGACG-3' Arch-amoAR: 5'-GCGGCCATCCATCTGTATGT-3'	Cloning	95 ºC/5 min, (94 ºC/45 s, 53 ºC/60 s, 72 ºC/60 s) x 30, 72 ºC /900 s.	Francis *et al*., 2005 Dang *et al*., 2010
MGI 16S rRNA	GI_751F: 5′-GTCTACCAGAACAYGTTC-3' GI_956R: 5′-HGGCGTTGACTCCAATTG-3'	qPCR	95 ºC/15 min, (95 ºC/5 s, 58 ºC/30 s, 72 ºC/40 s) x 40.	Mincer *et al*., 2007
pSL12 16S rRNA	pSL12_750F: 5′-GGTCCRCCAGAACGCGC-3' pSL12_876R: 5′-GTACTCCCCAGGCGGCAA-3'	qPCR	95 ºC/2 min, (95 ºC/5 s, 65 ºC/30 s, 72 ºC/32 s) x 40.	Mincer *et al*., 2007
Thaumarchaeota *hcd*	hcd-911F: 5'-AGCTATGTBTGCAARACAGG-3' hcd-1267R: 5'-CTCATTCTGTTTTCHACATC-3'	qPCR	95 ºC/2 min, (95 ºC/5 s, 55 ºC/30 s, 72 ºC/35 s) x 40.	Offre *et al*., 2011
Thaumarchaeota *amoA*	Arch-amoAF: 5'-STAATGGTCTGGCTTAGACG-3' Arch-amoAR: 5'-GCGGCCATCCATCTGTATGT-3'	qPCR	95 ºC/15 min, (95 ºC/10 s, 56 ºC/20 s, 72 ºC/30 s) x 40.	Francis *et al*., 2005 Dang *et al*., 2010
Betaproteobacteria *amoA*	amoA-1F*: 5'-GGGGHTTYTACTGGTGGT-3' amoA-2R: 5'-CCCCTCKGSAAAGCCTTCTTC-3'	qPCR	95 ºC/2 min, (95 ºC/5 s, 56 ºC/20 s, 72 ºC/30 s) x 40.	Stephen *et al*., 1999 Dang *et al*., 2010

REFERENCES

1. **Dang HY, Luan XW, Chen RP, Zhang XX, Guo LZ, Klotz MG.** 2010. Diversity, abundance and distribution of *amoA*-encoding archaea in deep-sea methane seep sediments of the Okhotsk Sea. FEMS Microbiol. Ecol. **72:**370-385.
2. **Francis CA, Roberts KJ, Beman JM, Santoro AE, Oakley BB.** 2005. Ubiquity and diversity of ammonia-oxidizing archaea in water columns and sediments of the ocean. Proc. Natl. Acad. Sci. U. S. A. **102:**14683-14688.
3. **Mincer YJ, Church MJ, Taylor LT, Preston C, Karl DM, DeLong EF.** 2007. Quantitative distribution of presumptive archaeal and bacterial nitrifiers in Monterey Bay and the North Pacific Subtropical Gyre. Environ. Microbiol. **9:**1162-1175.
4. **Offre P, Nicol GW, Prosser JI.** 2011. Community profiling and quantification of putative autotrophic thaumarchaeal communities in environmental samples. Environ. Microbiol. Rep. **3:**245-253.
5. **Stephen JR, Chang YJ, Macnaughton SJ, Kowalchuk GA, Leung KT, Flemming CA, White DC.** 1999. Effect of toxic metals on indigenous soil β-subgroup proteobacterium ammonia oxidizer community structure and protection against toxicity by inoculated metal-resistant bacteria. Appl. Environ. Microbiol. **65:**95-101.

Table S3. Efficiency and sensitivity of individual qPCR standard curve determined via plasmid DNA.

Target gene	Primer set	Efficiency			Sensitivity (copy number/µl plasmid DNA)	
		R^2	Slope	Linearity range	Expected value	Obtained value
MGI 16S rRNA	GI_751F, GI_956R	0.997	-3.248	10^1-10^5	3.63×10^4	3.75×10^4
pSL12 16S rRNA	pSL12_750F, pSL12_876R	0.991	-3.273	10^0-10^9	2.96×10^4	3.02×10^4
Archaeal *hcd*	hcd-911F, hcd-1267R	0.990	-3.316	10^1-10^{10}	2.88×10^4	2.89×10^4
Archaeal *amoA*	Arch-amoAF, Arch-amoAR	0.994	-3.231	10^0-10^9	2.68×10^4	2.79×10^4
Bacterial *amoA*	amoA-1F*, amoA-2R	0.998	-3.467	10^1-10^6	9.45×10^4	8.88×10^4

Table S4. Diversity and predicted richness of the sediment thaumarchaeotal *amoA* gene sequences obtained from the nSCS.

Station	No. of clones	No. of unique gene sequences[a]	No. of OTUs[b]	*C* (%)	*H*	1/*D*	*J*	S_{ACE}	S_{Chao1}
A3	328	56	33	97.0	3.35	5.26	0.66	46.26	36.75
CF6	109	34	23	91.7	3.52	6.60	0.78	32.22	32.00
CF8	100	24	15	94.0	2.53	3.54	0.65	20.09	18.75
CF11	84	27	16	94.0	2.75	3.60	0.69	19.98	18.00
CF14	123	38	27	87.8	3.58	7.56	0.75	70.92	44.50
CF15	92	22	14	95.7	3.15	7.34	0.83	18.20	16.00
E407	114	31	24	93.9	3.53	6.70	0.77	31.80	26.10
E422	91	20	9	96.7	2.07	3.35	0.65	11.57	10.00
E501	93	33	25	90.3	3.84	9.32	0.83	32.29	29.50
E504	97	29	22	89.7	3.08	4.37	0.69	37.84	27.63
E505	109	27	19	93.6	3.40	7.92	0.80	29.66	23.20
E801	117	34	27	88.9	3.73	8.42	0.78	49.02	40.00

[a] Unique gene sequences were defined by the RFLP molecular technique detailed in previous publications (Dang *et al*., 2009, 2010).

[b] OTUs of the thaumarchaeotal *amoA* sequences were determined at 0.05 distance cutoff using the DOTUR program. The coverage (*C*), Shannon-Weiner (*H*), Simpson (*D*) and evenness (*J*) indices, and S_{ACE} and S_{Chao1} richness estimators were calculated using the OTUs data.

REFERENCES

1. **Dang H, Li J, Zhang X, Li T, Tian F, Jin W.** 2009. Diversity and spatial distribution of *amoA*-encoding archaea in the deep-sea sediments of the tropical West Pacific Continental Margin. J. Appl. Microbiol. **106:**1482-1493.
2. **Dang HY, Luan XW, Chen RP, Zhang XX, Guo LZ, Klotz MG.** 2010. Diversity, abundance and distribution of *amoA*-encoding archaea in deep-sea methane seep sediments of the Okhotsk Sea. FEMS Microbiol. Ecol. **72:**370-385.

Table S5. Pearson correlation analyses of the key microbial abundance with measured environmental factors.

Gene Abundance or ratio	Pearson correlation coefficient (*p* value)[a]												
	Depth (m)	Temperature (ºC)	Salinity (‰)	DO (μM)	NO_3^- (μM)	NO_x^- (μM)	OrgC (%)	OrgN (%)	OrgC/OrgN	WC (%)	Silt (%)	Clay (%)	Skew
MGI 16S rRNA	-0.528 (0.078)	0.249 (0.435)	0.218 (0.496)	-0.351 (0.263)	-0.202 (0.529)	-0.200 (0.534)	0.214 (0.505)	0.182 (0.572)	-0.095 (0.770)	0.047 (0.884)	**0.729 (0.007)**	-0.271 (0.394)	0.253 (0.428)
pSL12 16S rRNA	0.161 (0.617)	-0.474 (0.120)	0.003 (0.992)	0.134 (0.677)	-0.137 (0.672)	-0.127 (0.693)	**0.653 (0.021)**	**0.695 (0.012)**	-0.412 (0.184)	0.332 (0.291)	0.068 (0.833)	0.287 (0.366)	-0.037 (0.909)
Thaumarchaeotal *hcd*	**-0.583 (0.047)**	0.536 (0.072)	0.177 (0.582)	-0.554 (0.062)	-0.265 (0.405)	-0.218 (0.496)	-0.096 (0.767)	-0.173 (0.590)	0.261 (0.413)	0.224 (0.484)	0.497 (0.100)	-0.303 (0.338)	0.202 (0.528)
Thaumarchaeotal *amoA*	-0.529 (0.077)	0.447 (0.145)	0.352 (0.262)	**-0.595 (0.041)**	-0.465 (0.128)	-0.421 (0.173)	-0.165 (0.609)	-0.154 (0.633)	-0.003 (0.992)	0.042 (0.896)	0.561 (0.058)	-0.372 (0.234)	0.279 (0.379)
Betaproteobacterial *amoA*	-0.424 (0.169)	0.358 (0.253)	0.070 (0.828)	-0.429 (0.164)	0.082 (0.799)	0.079 (0.806)	0.450 (0.142)	0.326 (0.302)	0.228 (0.477)	**0.677 (0.015)**	0.271 (0.395)	0.086 (0.789)	0.041 (0.900)
Thaumarchaeotal *amoA*/16S rRNA	**-0.601 (0.039)**	0.547 (0.066)	0.324 (0.305)	**-0.781 (0.003)**	**-0.661 (0.019)**	**-0.639 (0.025)**	-0.297 (0.348)	-0.222 (0.488)	-0.106 (0.743)	-0.104 (0.748)	0.237 (0.457)	-0.568 (0.054)	0.472 (0.121)
Thaumarchaeotal *hcd*/16S rRNA	-0.384 (0.218)	**0.673 (0.017)**	0.036 (0.911)	-0.425 (0.169)	-0.193 (0.547)	-0.171 (0.595)	**-0.579 (0.048)**	**-0.644 (0.024)**	0.502 (0.096)	0.006 (0.984)	-0.251 (0.432)	-0.390 (0.211)	0.168 (0.601)
Thaumarchaeotal *hcd*/*amoA*	0.491 (0.105)	-0.358 (0.253)	-0.115 (0.722)	**0.669 (0.017)**	**0.833 (0.001)**	**0.836 (0.001)**	-0.048 (0.882)	-0.183 (0.570)	**0.646 (0.023)**	0.250 (0.433)	-0.370 (0.236)	**0.578 (0.049)**	**-0.822 (0.001)**
Archaea/Bacteria *amoA*	-0.528 (0.078)	0.467 (0.125)	**0.622 (0.031)**	-0.387 (0.214)	-0.428 (0.165)	-0.432 (0.161)	-0.396 (0.202)	-0.323 (0.306)	-0.215 (0.502)	-0.514 (0.087)	**0.667 (0.018)**	-0.558 (0.059)	0.396 (0.202)
Crenarchaeol abundance	0.419 (0.175)	**-0.581 (0.047)**	-0.214 (0.505)	0.086 (0.790)	-0.118 (0.714)	-0.161 (0.618)	**0.723 (0.008)**	**0.773 (0.003)**	-0.527 (0.078)	0.493 (0.103)	0.206 (0.520)	0.372 (0.234)	-0.022 (0.945)
BIT	-0.098 (0.762)	0.306 (0.334)	0.285 (0.369)	0.098 (0.763)	0.506 (0.094)	0.503 (0.095)	-0.449 (0.143)	**-0.591 (0.043)**	**0.848 (0.000)**	0.048 (0.883)	-0.342 (0.277)	0.133 (0.679)	-0.550 (0.064)

[a] The **yellow-colored** boxes show the *p* values that are significant (≤0.05) for the positive correlations and the **blue-colored** boxes show the *p* values that are significant (≤0.05) for the negative correlations.

Table S6. Archaeal and bacterial core lipid data for the 12 sediment samplings collected from the nSCS[a].

	Archaeal core lipid *i*GDGTs (ng/g sediment)							Bacterial core lipid *b*GDGTs (ng/g sediment)								
	GDGT-0	GDGT-1	GDGT-2	GDGT-3	GDGT-4	Cren.	Cren.iso.	GDGT-III	GDGT-IIIb	GDGT-IIIc	GDGT-II	GDGT-IIb	GDGT-IIc	GDGT-I	GDGT-Ib	GDGT-Ic
A3	106.48	28.69	20.17	8.24	3.59	380.19	6.78	4.39	0.00	0.00	15.61	3.65	1.15	18.40	7.54	6.01
CF6	207.32	58.89	75.54	12.87	3.05	566.31	47.87	5.42	0.00	0.00	9.17	3.64	0.94	16.81	4.34	2.07
CF8	226.65	65.96	82.31	13.00	0.68	639.96	51.19	7.04	0.00	0.00	5.97	3.59	1.46	7.19	2.42	1.85
CF11	226.77	64.64	79.27	13.28	5.58	575.63	47.52	9.89	0.00	0.00	3.98	4.43	1.76	5.88	2.20	1.70
CF14	277.82	78.47	91.49	14.58	1.48	684.42	57.45	11.85	0.00	0.00	4.06	4.55	1.93	5.87	2.23	1.65
CF15	279.36	81.56	102.62	15.91	0.47	725.78	60.61	14.88	0.00	0.00	5.28	4.93	2.08	5.74	2.25	1.36
E407	79.51	22.82	28.88	4.30	1.08	200.61	17.57	5.06	0.00	0.00	5.15	2.23	1.06	20.31	2.83	1.19
E422	166.80	49.33	56.84	10.42	0.05	469.95	36.24	8.19	0.00	0.00	6.69	3.69	1.60	7.71	2.52	1.89
E501	49.37	15.08	10.74	4.28	1.46	186.83	3.77	1.85	0.00	0.00	5.51	1.48	0.58	6.72	3.36	2.66
E504	80.94	28.84	25.93	9.55	2.83	329.19	11.83	3.39	0.00	0.87	7.27	2.59	1.07	7.89	4.58	3.84
E505	58.02	21.22	21.16	7.46	0.32	240.46	11.40	2.83	0.00	0.81	5.39	1.97	0.80	4.58	2.56	2.30
E801	84.72	32.89	29.81	6.09	0.00	288.02	21.69	6.09	0.63	0.00	3.88	2.65	0.83	6.27	1.52	1.39

[a] Sediment membrane core lipid analyses have been performed previously (Ge *et al*., 2012), except for the data of sampling station E801 that were determined in this study.

REFERENCE

Ge HM, Zhang CL, Dang HY, Zhu C, Jia GD. 2012. Distribution of tetraether lipids in surface sediments of the northern South China Sea: Implications for TEX_{86} proxies. Geosci. Front. Accepted, in press. DOI: 10.1016/j.gsf.2012.10.002.

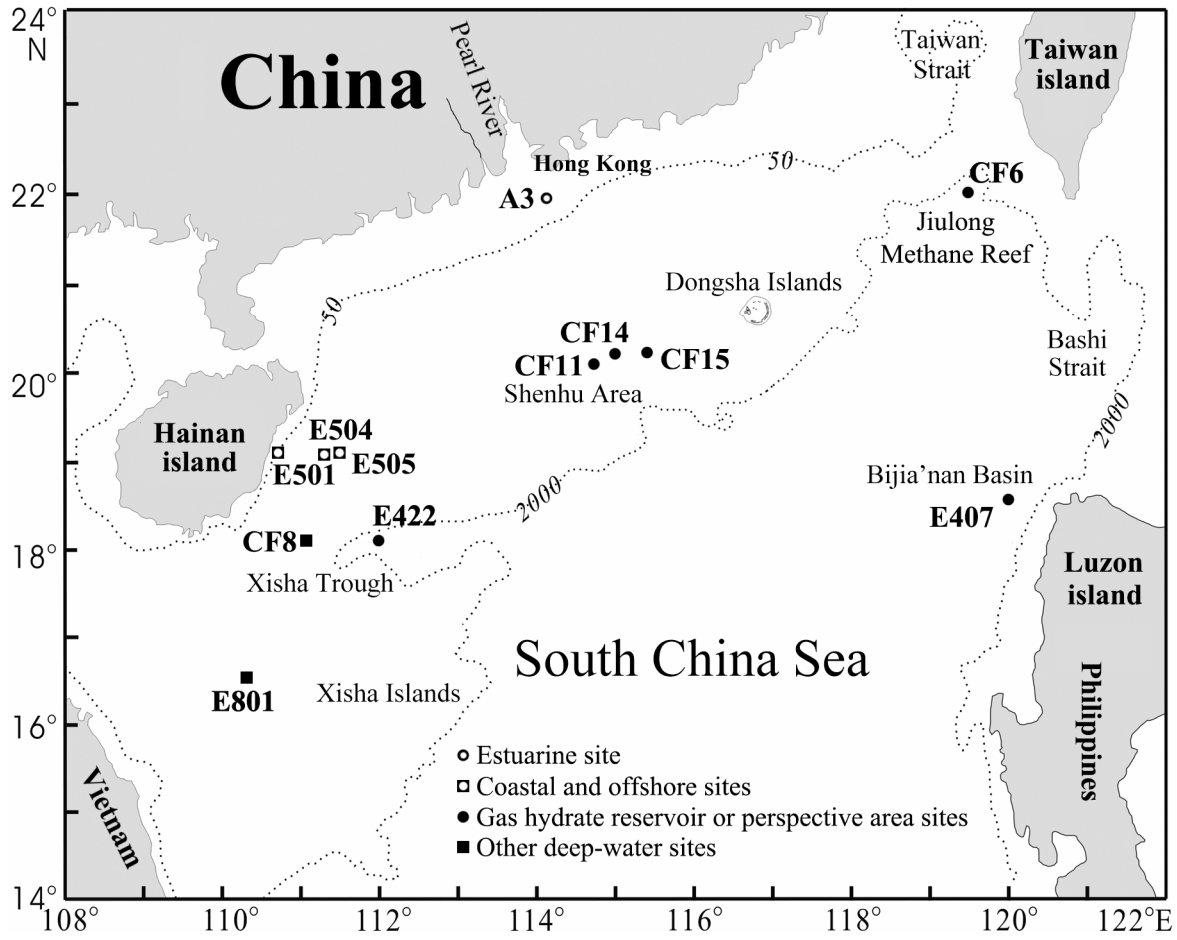

Fig. S1. Map showing the 12 surface sediment sampling sites in the northern South China Sea, modified from Zhou *et al*. (2009) (With kind permission from Springer Science+Business Media: Microbial Ecology, Diversity of both the cultivable protease-producing bacteria and their extracellular proteases in the sediments of the South China Sea, vol. 58, 2009, p. 582-590, M.-Y. Zhou, X.-L. Chen, H.-L. Zhao, H.-Y. Dang, X.-W. Luan, X.-Y. Zhang, H.-L. He, B.-C. Zhou, and Y.-Z. Zhang, Fig. 1.) and Dang *et al*. (2013).

REFERENCES

1. **Dang HY, Yang JY, Li J, Luan XW, Zhang YB, Gu GZ, Xue RR, Zong MY, Klotz MG.** 2013. Environment-dependent distribution of the sediment *nifH*-harboring microbiota in the northern South China Sea. Appl. Environ. Microbiol. **79:**121-132.
2. **Zhou MY, Chen XL, Zhao HL, Dang HY, Luan XW, Zhang XY, He HL, Zhou BC, Zhang YZ.** 2009. Diversity of both the cultivable protease-producing bacteria and their extracellular proteases in the sediments of the South China Sea. Microb. Ecol. **58:**582-590.

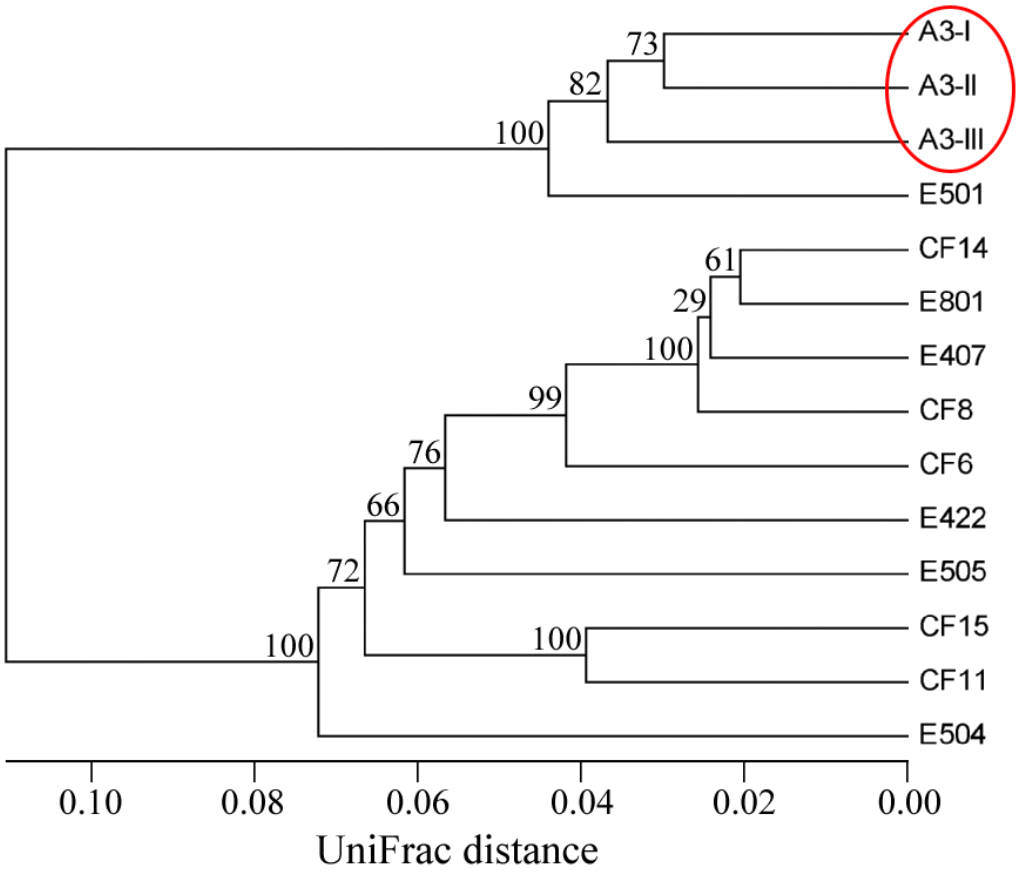

Fig. S2. Dendrogram of the hierarchical clustering analysis of the nSCS sediment AEA assemblages constructed with the Fast UniFrac normalized and weighted Jackknife Environment Clusters statistical method. The three *amoA* gene clone libraries of the A3-I, A3-II and A3-III sediment subcore samples of the A3 station are grouped together, indicating the high similarity of the respective clone libraries of the replicate subcore sediment samples at this station.

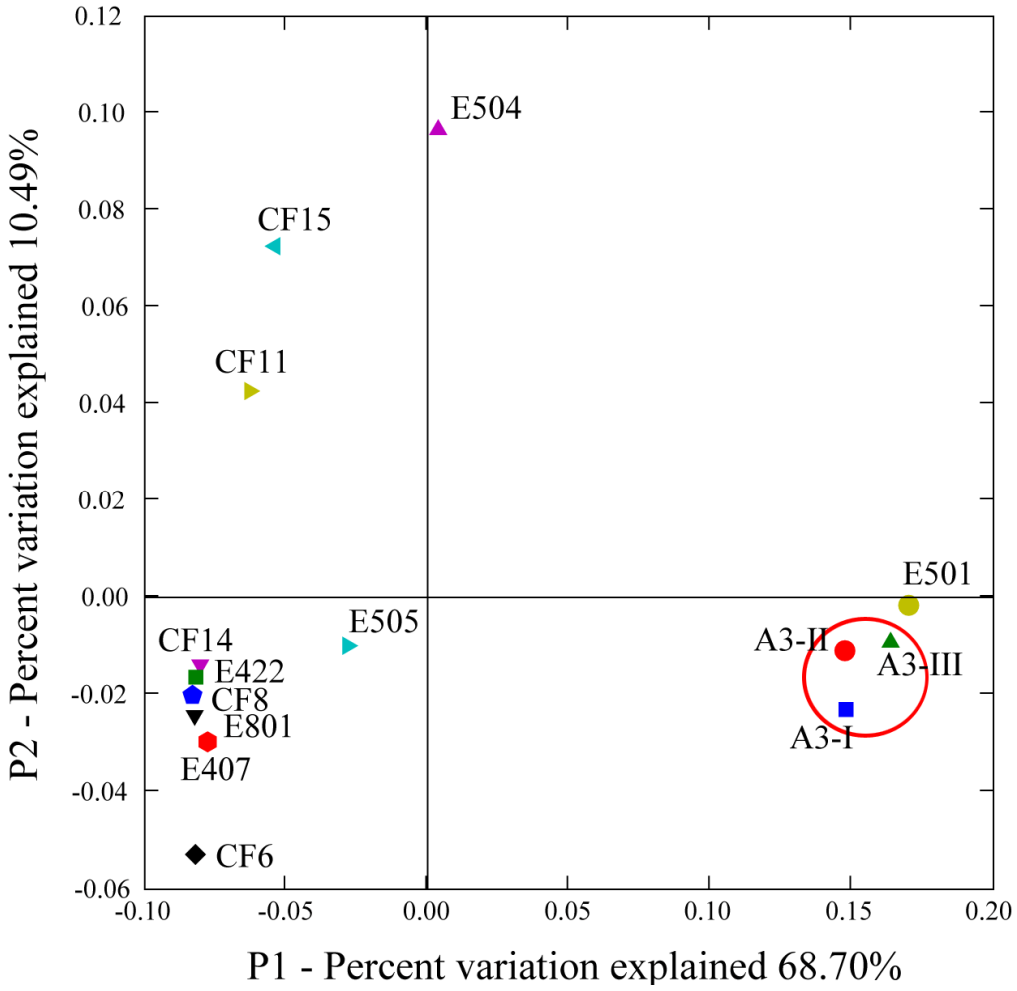

Fig. S3. Ordination diagram of the Fast UniFrac weighted and normalized PCoA analysis of the nSCS sediment AEA assemblages. The three *amoA* clone libraries of the A3-I, A3-II and A3-III sediment subcore samples of station A3 are located very closely to each other in this diagram, indicating the high similarity of the respective clone libraries of the replicate subcore sediment samples at this station.

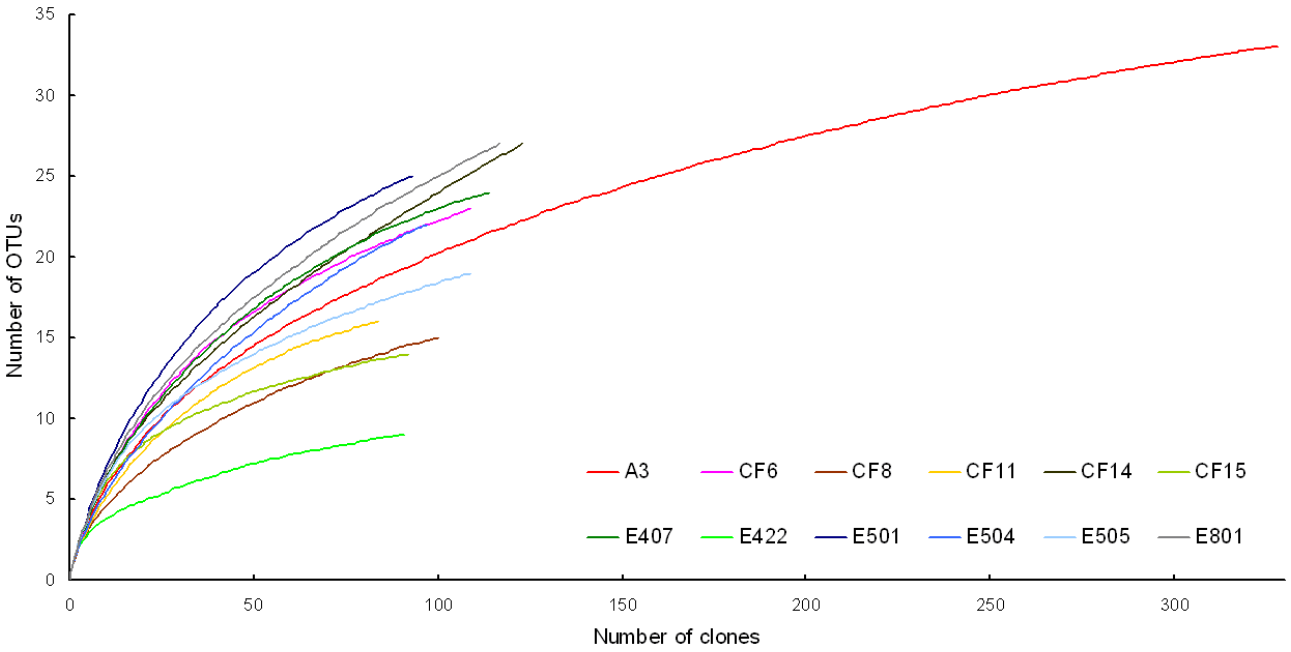

Fig. S4. Rarefaction curves of the OTUs in the archaeal *amoA* gene clone libraries constructed with the marine sediment samples collected from the nSCS.

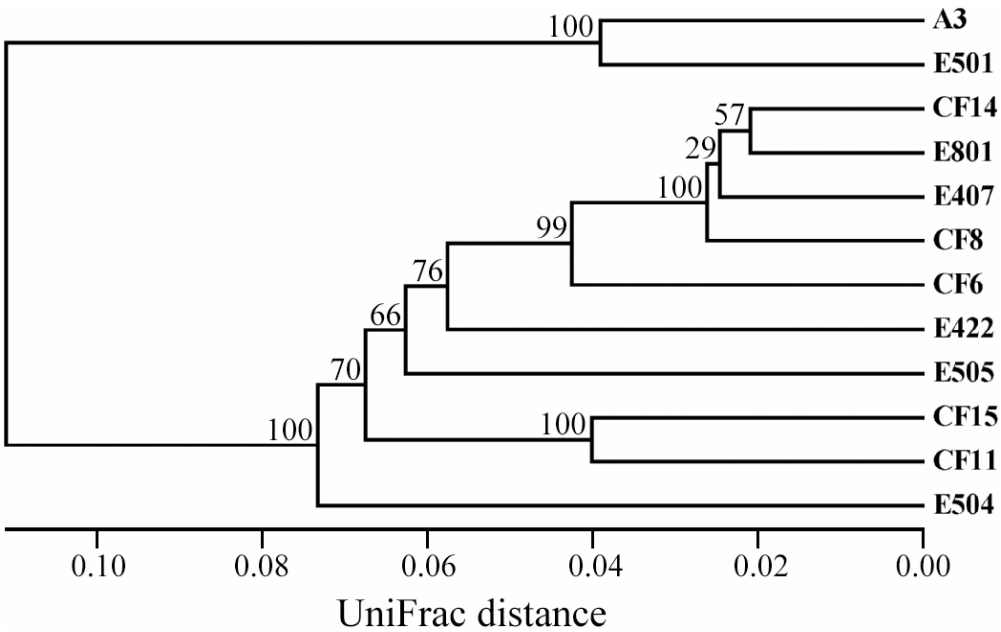

Fig. S5. Dendrogram of the hierarchical clustering analysis of the nSCS sediment AEA assemblages constructed using the Fast UniFrac weighted Jackknife Environment Clusters statistical method. The percentage supports of the classification tested with sequence jackknifing resamplings are shown near the corresponding nodes.

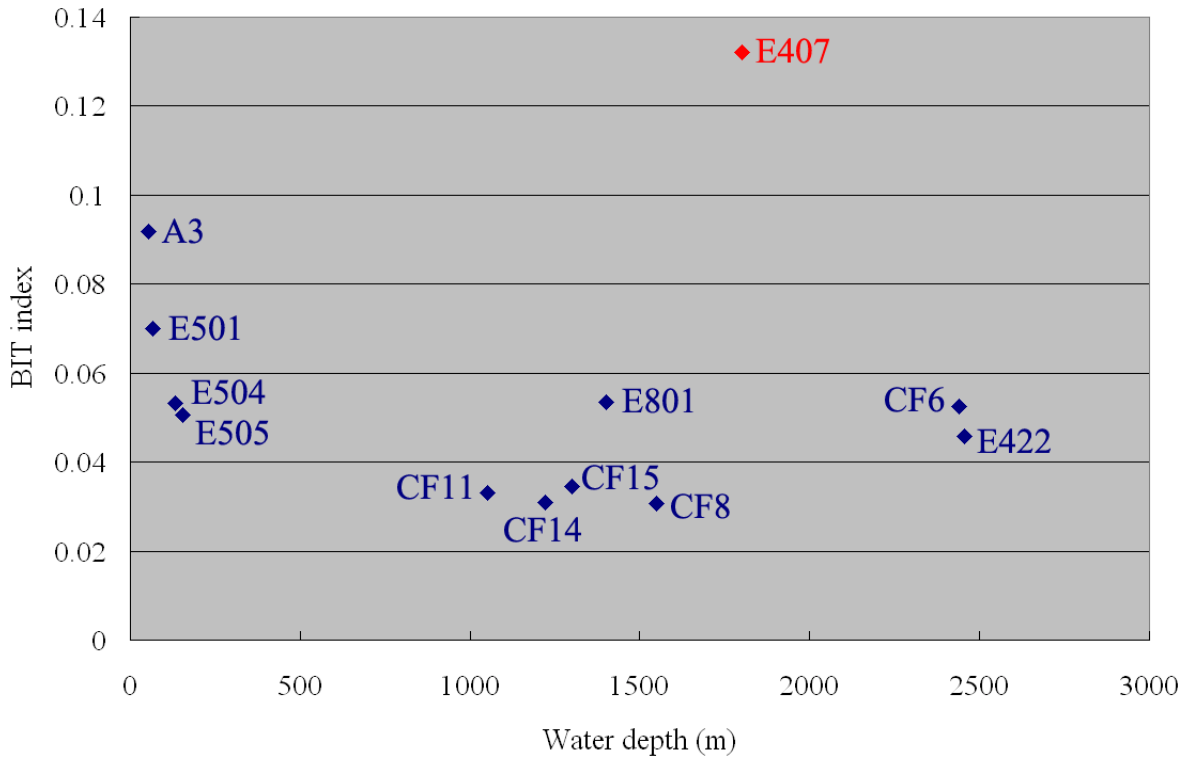

Fig. S6. The distribution of the BIT values in the different nSCS sampling sites with reference to the water depth at the sampling sites using the archaeal and bacterial membrane core lipid data collected from the current and a previous study (Ge *et al*., 2012).

REFERENCE

Ge HM, Zhang CL, Dang HY, Zhu C, Jia GD. 2012. Distribution of tetraether lipids in surface sediments of the northern South China Sea: Implications for TEX_{86} proxies. Geosci. Front. Accepted, in press. DOI: 10.1016/j.gsf.2012.10.002.

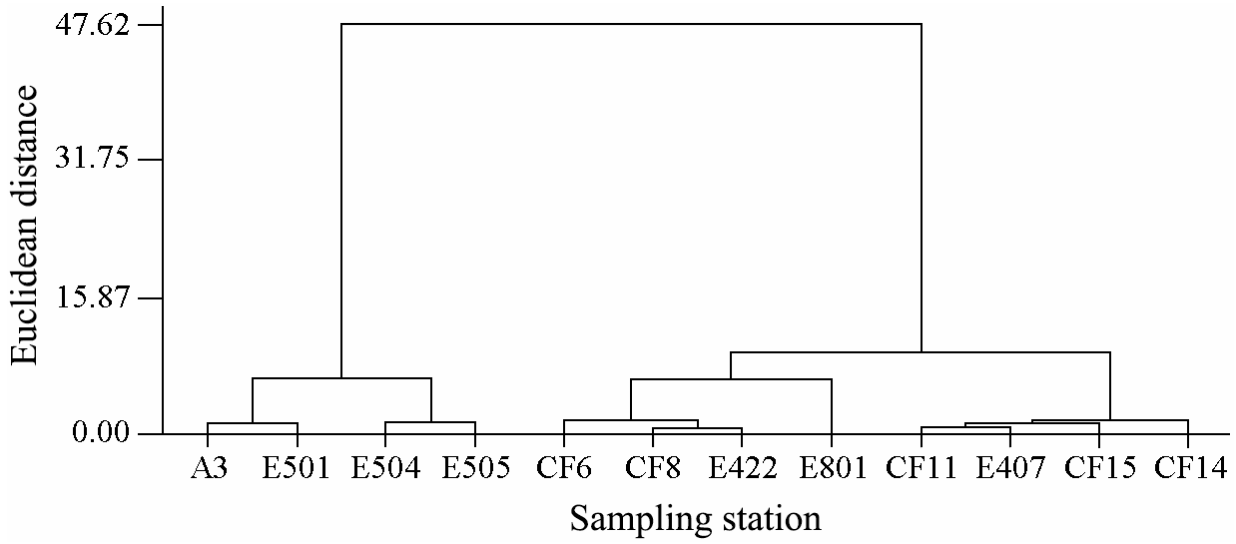

Fig. S7. Dendrogram of the hierarchical clustering analysis of the nSCS sediment putative fossil archaeal assemblages constructed using the archaeal membrane core lipid data collected from the current and a previous study (Ge *et al*., 2012).

REFERENCE

Ge HM, Zhang CL, Dang HY, Zhu C, Jia GD. 2012. Distribution of tetraether lipids in surface sediments of the northern South China Sea: Implications for TEX_{86} proxies. Geosci. Front. Accepted, in press. DOI: 10.1016/j.gsf.2012.10.002.

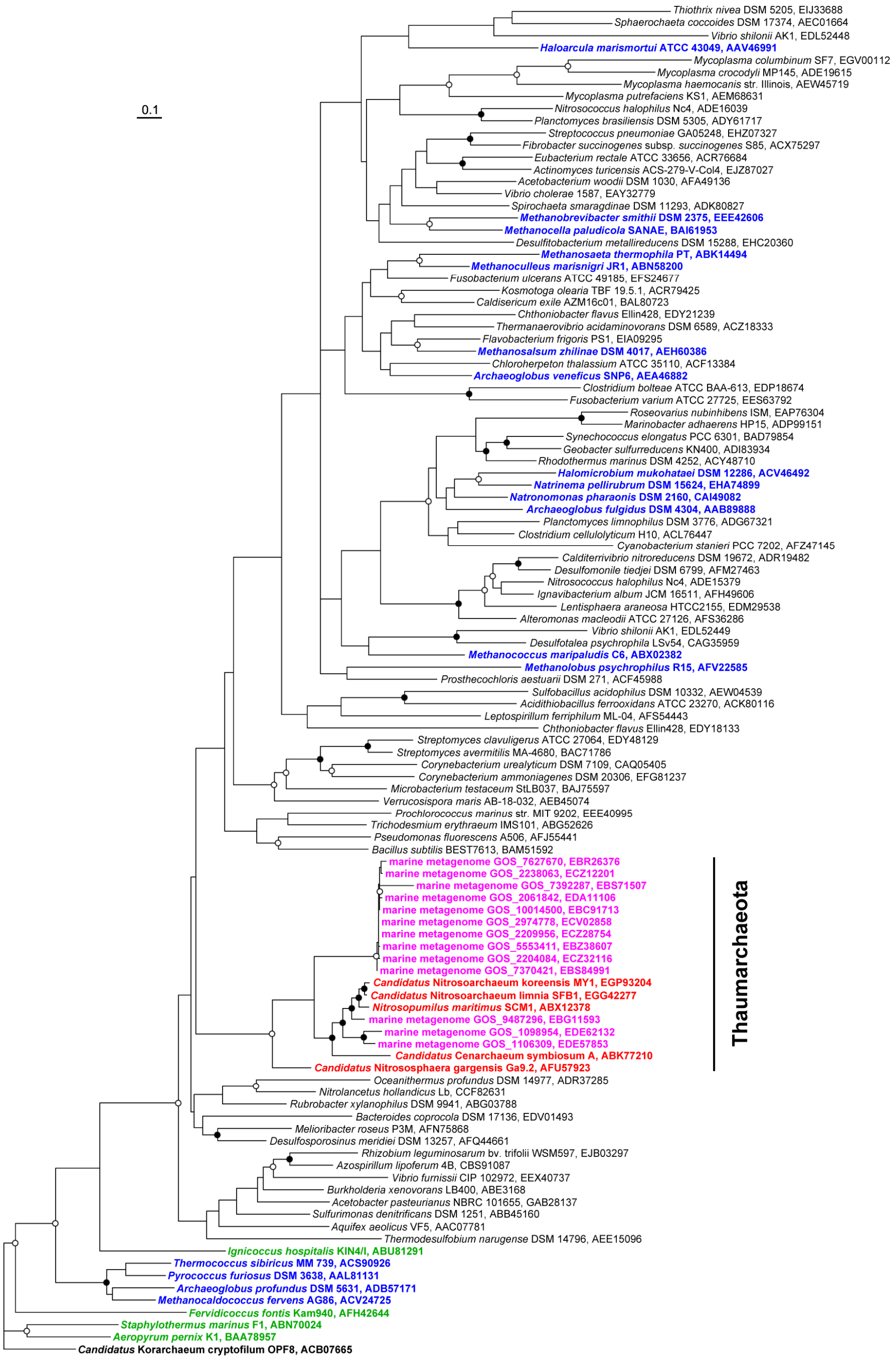

Fig. S8. Consensus phylogenetic tree of the permease inner membrane protein PstA subunit sequences of the microbial high-affinity, high-activity phosphate-specific ABC transporter systems. The PstA sequences were retrieved from GenBank and analyzed by using distance neighbor-joining inference. Archaeal PstA sequences were denoted with bold fonts, with Thaumarchaeota sequences being labeled with red (from genomes) or purple (from metagenomes) color and Crenarchaeota and Euryarchaeota sequences being labeled with green or blue color, respectively. The Korarchaeota PstA sequence affiliated to *Ca*. Korarchaeum cryptofilum was used as the outgroup. Bootstrap values (100 resamplings) no less than 70% are shown with solid circle symbols and those less than 70% but greater than or equal to 50% are shown with open circle symbols near the corresponding nodes.